ACCOUNTS
of chemical research

Third Generation Photovoltaics based on Multiple Exciton Generation in Quantum Confined Semiconductors

MATTHEW C. BEARD,*,† JOSEPH M. LUTHER,†
OCTAVI E. SEMONIN,†,‡ AND ARTHUR J. NOZIK†,§

†National Renewable Energy Laboratory, Golden, Colorado 80401, United States, ‡Department of Physics, University of Colorado, Boulder, Colorado 80309, United States, and §Department of Chemistry and Biochemistry, University of Colorado, Boulder, Colorado 80309, United States

RECEIVED ON JULY 2, 2012

CONSPECTUS

Improving the primary photoconversion process in a photovoltaic cell by utilizing the excess energy that is otherwise lost as heat can lead to an increase in the overall power conversion efficiency (PCE). Semiconductor nanocrystals (NCs) with at least one dimension small enough to produce quantum confinement effects provide new ways of controlling energy flow not achievable in thin film or bulk semiconductors. Researchers have developed various strategies to incorporate these novel structures into suitable solar conversion systems. Some of these methods could increase the PCE past the Shockley–Queisser (SQ) limit of ~33%, making them viable "third generation photovoltaic" (TGPV) cell architectures. Surpassing the SQ limit for single junction solar cells presents both a scientific and a technological challenge, and the use of semiconductor NCs to enhance the primary photoconversion process offers a promising potential solution.

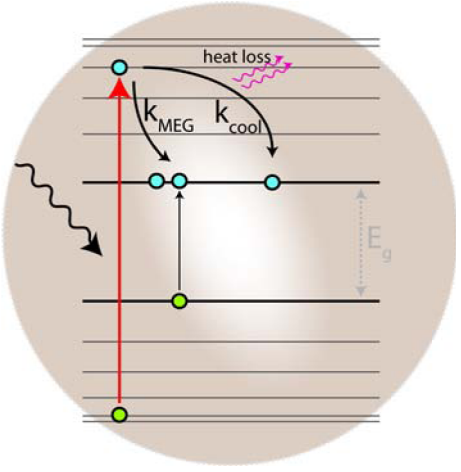

The NCs are synthesized via solution phase chemical reactions producing stable colloidal solutions, where the reaction conditions can be modified to produce a variety of shapes, compositions, and structures. The confinement of the semiconductor NC in one dimension produces quantum films, wells, or discs. Two-dimensional confinement leads to quantum wires or rods (QRs), and quantum dots (QDs) are three-dimensionally confined NCs. The process of multiple exciton generation (MEG) converts a high-energy photon into multiple electron–hole pairs. Although many studies have demonstrated that MEG is enhanced in QDs compared with bulk semiconductors, these studies have either used ultrafast spectroscopy to measure the photon-to-exciton quantum yields (QYs) or theoretical calculations. Implementing MEG in a working solar cell has been an ongoing challenge.

In this Account, we discuss the status of MEG research and strategies towards implementing MEG in working solar cells. Recently we showed an external quantum efficiency for photocurrent of greater than 100% (reaching 114%) at ~4E_g in a PbSe QD solar cell. The internal quantum efficiency reached 130%. These results compare favorably with ultrafast transient spectroscopic measurements. Thus, we have shown that one of the tenets of the SQ limit, that photons only produce one electron–hole pair at the electrodes of a solar cell, can be overcome. Further challenges include increasing the MEG efficiency and improving the QD device structure and operation.

Introduction

Third generation photovoltaic (PV) solar cells have two defining characteristics: (1) a power conversion efficiency greater than the Shockley–Queisser (SQ) limit of 33%[1] and (2) a low cost per unit area. According to Green,[2] in order to be classified as a third generation PV (TGPV) cell, the cost of the PV module, $/unit area, divided by the watts delivered/unit area should yield a price per peak watt (W_p) for the module of about $0.20 US. Any combination of efficiency and areal cost yielding $0.20/$W_p$ or below would be

Published on the Web 10/31/2012 www.pubs.acs.org/accounts
10.1021/ar3001958

classified as a TGPV technology. For example, a PV module having a cost of \$100/m^2 delivering 500 W/m^2 could achieve this goal. To obtain the yearly averaged energy cost for the PV system (\$/(kW·h)), various factors need consideration: the balance of systems (BOS) cost, the module cost and its useful life, the averaged annual-capacity factor for the PV system, and finally, other operating costs such as interest rates, maintenance, and taxes; for example, a simple, but rough, conversion is to multiply the total \$/W_p cost (module + BOS) by 0.04 to 0.05 (depending upon geographical location) to obtain \$/(kW·h). If the module and BOS costs remain about equal, as they are today, then a \$0.20/W_p module cost would result in a total system cost of \$0.40/W_p achieving an energy cost of about \$0.02/(kW·h), a cost comparable to coal or natural gas. To achieve 500 W/m^2, a module efficiency of 50% is required (the average solar irradiance is 1 kW/m^2), well above the SQ limit.

Over the past few years, we have investigated the TGPV concept of multiple exciton generation (MEG) in quasi-spherical semiconductor nanocrystals or quantum dots (QDs). We have mainly focused on PbSe QDs because quantum confinement effects are particularly strong.[3] The bandgap can be continuously tuned from ~0.5 to 2 eV by spanning a reasonable size range of 1−10 nm. When a photon of sufficient energy is absorbed by a QD, an electron−hole (e−h) pair is produced. The lowest absorbing state in a QD is generally termed the first exciton state (and defined as the bandgap), where excitons are e−h pairs that interact through the Coulomb potential. Excitons in confined semiconductors differ from excitons in bulk semiconductors because the e−h pairs are confined to small regions of space defined by the dimensions of the structure and therefore continue to interact, whereas in bulk semiconductors, excitons are only present if k_BT is lower than the exciton binding energy (typically only a few millielectronvolts).

If the incident photon energy is greater than E_g then higher energy states absorb the photon to produce a "hot exciton" with excess energy, $\Delta E_{ex} = h\nu - E_g$. In semiconductors, the excess energy prior to cooling is converted into kinetic energy, and if $\Delta E_{ex} > E_g$ ($h\nu > 2E_g$), then it can be used to produce one or more extra e−h pairs. This avenue was investigated in bulk semiconductors (termed impact ionization, Figure 1)[4,5] for many years but was ultimately deemed too inefficient to have a significant impact on PV.[6] In bulk semiconductors, two factors reduce the likelihood that hot carriers will undergo impact ionization; the density of final states is limited by crystal momentum, which must be conserved between the initial and final states, and rapid

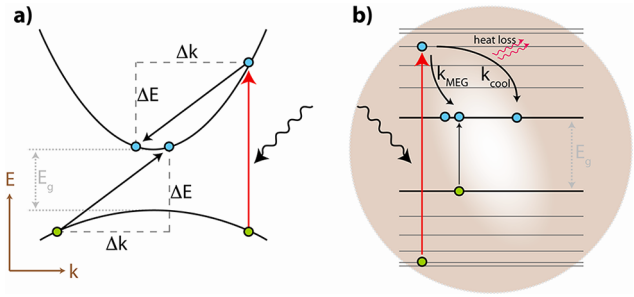

FIGURE 1. (a) Schematic depiction of impact ionization in a bulk semiconductor; both energy and crystal momentum must be conserved, as shown. (b) MEG in a quantum-confined structure such as a QD, which has small dimensions and thus Bloch states with defined momentum are not eigenstates, such that only energy needs to be conserved. Hot carriers undergo one of two competing processes: (1) generation of an extra e−h pair (k_{MEG}) or (2) cooling of the single exciton state (k_{cool}).

hot carrier cooling via phonon emission to the band edge (~1 ps or less) can compete efficiently with impact ionization. The result is that impact ionization does not produce multiple e−h pairs until $h\nu > (4-5)E_g$. QDs offer ways to overcome these limitations. In QDs, only energy conservation sets fundamental limits on MEG because crystal momentum is a result of long-range repeating atomic potentials, which are not present in QDs. Hot-carrier relaxation can be modified in QD systems[7−9] so that MEG can better compete. Finally, carrier−carrier interactions are larger due to the physical confinement within the QD. The added degrees of freedom afforded by quantum-confined semiconductors (shape, size, composition, surface engineering, etc.) allow for tailoring key parameters to potentially revolutionize PV.

MEG Efficiency and Hot-Exciton Cooling

Ultrafast transient absorption (TA) spectroscopy (Figure 2) or time-resolved photoluminescence (TRPL) is typically employed to study MEG in colloidal solutions of isolated QDs.[10−13] The evidence that multiple excitons are produced per absorbed photon is the appearance of a fast multiexciton decay component in the transient dynamics due to rapid Auger recombination when photoexcited above the energy conservation threshold ($h\nu > 2E_g$); the experiments are performed with conditions such that each QD absorbs either zero or one photon. The number of e−h pairs created per absorbed photon (the exciton quantum yield, QY) can be obtained by analyzing the amplitude of the single- and multiexciton components (single exciton lifetimes are typically much greater than multiexciton lifetimes). There has been debate[14−19] over TA measurements because of the

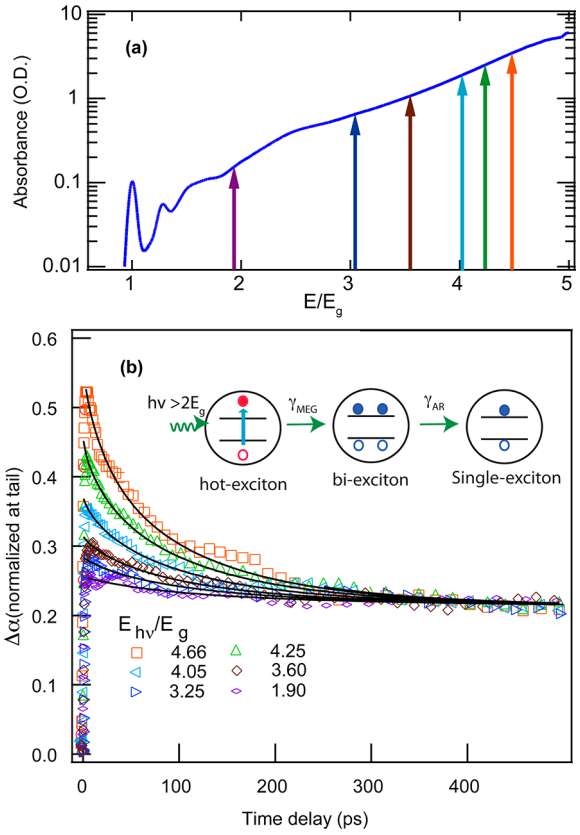

FIGURE 2. MEG transient absorption experiment. Part a is the linear absorption (plotted on a log scale vs E/Eg). Part b shows the transients for a constant excitation level but increasing photon energy shown in part a. The amplitude of the fast component increases with increasing photon energy indicative of increased biexciton yields. Reprinted with permission from ref 18. Copyright 2011 American Chemical Society.

large spread in reported QYs. Researchers concluded that some discrepancies and variations reported could be attributed to photocharging during the pulsed laser experiments.[19−21] Using lower fluences and rapidly flowing or stirring the solutions during the measurements can minimize or eliminate photocharging effects. We refer interested readers to several reviews of the MEG measurements that detail these complications.[13,18−20]

The number of e−h pairs generated per absorbed photon can be expressed by the following equation,[22]

$$\mathrm{QY} = 1 + \frac{k_{\mathrm{MEG}}}{(k_{\mathrm{MEG}}^{(1)} + k_{\mathrm{cool}})} + \frac{k_{\mathrm{MEG}}^{(1)} k_{\mathrm{MEG}}^{(2)}}{(k_{\mathrm{MEG}}^{(1)} + k_{\mathrm{cool}})(k_{\mathrm{MEG}}^{(2)} + k_{\mathrm{cool}})} + \cdots \quad (1)$$

where $k_{\mathrm{MEG}}^{(i)}$ is the rate of producing $(i+1)$ excitons from i hot excitons, and k_{cool} is the cooling rate. In deriving eq 1, we assume that the cooling rates of single- and multi-excitons are equivalent. Each successive term in eq 1 is only valid when energy conservation is met; thus when the photon energy is greater than $3E_g$, all three terms can contribute (this constraint is contained in the $k_{\mathrm{MEG}}^{(i)}$ term).[22] When $h\nu > 3E_g$, higher order terms are necessary and can be included by expanding the series. The photon energy where QY > 1 is the threshold energy ($h\nu_{\mathrm{th}}$).

To approximate how these rates change as a function of excess photon energy, we refer to work on impact ionization in bulk semiconductors where the rate of carrier cooling, k_{cool}, is fairly constant with excess energy.[23] In contrast, k_{MEG} increases with increasing energy above $h\nu_{\mathrm{th}}$.[24,25] Thus at high excess photon energy k_{MEG} and k_{cool} are related by[26]

$$k_{\mathrm{MEG}} = P k_{\mathrm{cool}} \left(\frac{h\nu_{\mathrm{ex}}}{h\nu_{\mathrm{th}}} \right)^2 \quad (2)$$

where $h\nu_{ex} = h\nu - h\nu_{\mathrm{th}}$, and P describes the competition between k_{MEG} and k_{cool} such that at a photon energy $h\nu = 2h\nu_{\mathrm{th}}$, $h\nu_{ex} = h\nu_{\mathrm{th}}$, and thus $k_{\mathrm{MEG}} = Pk_{\mathrm{cool}}$, (note that when $h\nu < h\nu_{\mathrm{th}}$, $k_{\mathrm{MEG}} = 0$). We find that the threshold photon energy for MEG is related to P by,

$$h\nu_{\mathrm{th}} = \left(2 + \frac{1}{P}\right) E_g = \left(2 + \frac{k_{\mathrm{cool}}}{k_{\mathrm{MEG}}^{2h\nu_{\mathrm{th}}}}\right) E_g \quad (3)$$

where $k_{\mathrm{MEG}}^{2h\nu_{\mathrm{th}}}$ is the MEG rate when $h\nu = 2h\nu_{\mathrm{th}}$. As $k_{\mathrm{MEG}}^{2h\nu_{\mathrm{th}}}$ increases or k_{cool} decreases, $h\nu_{\mathrm{th}}$ approaches the energy conservation limit of $2E_g$. We can also express these relationships in terms of the e−h pair creation energy, $\varepsilon_{\mathrm{eh}}$, which is the required excess energy to produce one additional e−h pair, $\varepsilon_{\mathrm{eh}} = \Delta h\nu/\Delta \mathrm{QY}$ for $h\nu > h\nu_{\mathrm{th}}$. In terms of $\varepsilon_{\mathrm{eh}}$, $h\nu_{\mathrm{th}}$ is given by $h\nu_{\mathrm{th}} = E_g + \varepsilon_{\mathrm{eh}}$. A MEG efficiency ($\eta_{\mathrm{MEG}}$) can be defined in terms $\varepsilon_{\mathrm{eh}}$ as $\eta_{\mathrm{MEG}} = E_g/\varepsilon_{\mathrm{eh}}$, and then $h\nu_{\mathrm{th}} = E_g + E_g/\eta_{\mathrm{MEG}}$.[22] Thus the number of e−h pairs produced and $h\nu_{\mathrm{th}}$ are related and will both improve if $k_{\mathrm{MEG}}/k_{\mathrm{cool}}$ is increased.

In Figure 3, we show QYs for bulk PbSe,[28] PbSe QDs,[19,21] and PbSe QRs.[29] *P* improves by a factor of 3 going from bulk PbSe to QDs of PbSe and an additional factor of 5 going to QRs, thus demonstrating that quantum confinement can help improve MEG. The QY is determined from spectroscopic measurements and plotted versus $h\nu/E_g$; we normalize the excitation photon energy to the bandgap so that the competition between MEG and cooling can be assessed directly (see eq 3). For the ideal case, where two e−h pairs are produced at exactly $2E_g$, three at $3E_g$, and so forth (the staircase scenario shown as the black line in Figure 3), *P* needs to exceed 10 000.

We adopt the terminology and notation of Baer and Rabani[30] to discuss factors that can increase k_{MEG} and thus

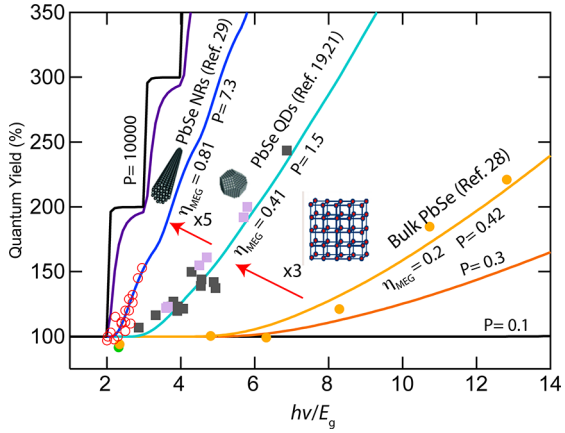

FIGURE 3. Quantum yield plot demonstrating the improvement in MEG for various dimensionalities of PbSe (bulk, spherical QDs, nanosized QRs). η_{MEG} determined following ref 22.

lead to a larger P. The total MEG rate, k_{MEG}, is the sum of the electron and hole multiplication rates ($k_{MEG} = \Gamma^{-} + \Gamma^{+}$). Within Fermi's golden rule approximation, $\Gamma^{-/+}$ is expressed as a product of the Coulomb interaction, $W_{e/h}$, and the density of positive or negative trion states ($\rho_T^{+/-}$),

$$\Gamma^{-/+} = (2\pi/\hbar)\langle W_{e/h}^2 \rangle \rho_T^{-/+} \quad (4)$$

Directly comparing this expression for quantum-confined and bulk semiconductors yields two conclusions: $W_{e/h}$ should be higher in quantum-confined nanostructures because the spatial confinement reduces the separation of carriers, and $\rho_T^{+/-}$ should be higher in QDs due to the relaxation of momentum conservation (thus more single exciton states can couple to trion states). Baer and Rabani find that Γ^{-} increases with decreasing QD size with a dependence of D^{-2},[30] where D is the diameter, while Lin et al. find a D^{-3} dependence.[31] While no calculations of MEG in QRs has been reported, Bartnik et al.[32] find a higher Coulomb interaction in the one-dimensional QR system, and this could explain the higher MEG values observed in the PbSe QRs compared to QDs.

A full quantum simulation based on the time-dependent density matrix method that goes beyond Fermi's golden rule approximation has recently been presented by Witzel et al.[33] and is an extension of the previous Shabaev–Efros–Nozik (SEN) coherent superposition model.[11,34] The SEN model describes MEG within the full multielectron Hamiltonian.[34] A coherent superposition of single- and multiexciton states that have nearly the same energy and are coupled through the multi-Coulomb interaction evolves from the initially populated one e–h pair state according to the time-dependent Schrödinger equation.[33]

TABLE 1. Common Approaches To Exceed the SQ Limit

approach	ideal PCE (%) at one-sun intensity
single junction[1]	33
tandem junctions[36]	
bilayer junction	42
triple	48
quadruple	53
5	55
infinite	68
intermediate band	47
up conversion[39]	48
down conversion[40]	40
MEG[41]	45
hot carrier[42]	67

A recent study[35] comparing PbS to PbSe QDs found that the MEG efficiency was lower in PbS compared with PbSe QDs even though the biexciton lifetime, which is governed by the same Coulomb matrix element, displayed similar behavior. Since k_{MEG} should be of a similar magnitude, the differences in the QYs result from differing k_{cool}. The differences in k_{cool} were rationalized by the bulk electron–phonon coupling parameter, α_F, which for PbS is 0.33 and for PbSe is 0.22. Thus one approach to further improve MEG is to explore quantum-confined semiconductors with smaller values of α_F.

High Efficiency Concepts for Solar Photoconversion

We now discuss how MEG can increase the theoretical power conversion efficiency. The ubiquitous Shockley and Queisser[1] (S–Q) analysis of the maximum thermodynamic efficiency of converting solar irradiance into electrical free energy in a single-junction PV cell assumes the following:

(1) Photons with energy less than E_g are not absorbed.
(2) Energetic electrons created by high-energy photons immediately relax to the band edge (i.e., the fraction of energy of photons with energy greater than E_g is immediately lost as heat).
(3) The solar cell radiates light as a blackbody, except below E_g, where the cell does not radiate.

Approaches to achieve higher theoretical efficiencies (Table 1) attempt to either use the high photon energies more efficiently or recover the low photon energies. The most developed approach is a multijunction or tandem junction solar cell employing a stack of p–n junctions where the light-absorbing semiconductor bandgap decreases in successive layers. In the limit of infinite junctions, the theoretical conversion efficiency reaches 68% at one-sun intensity.[36] Ross and Nozik[4] extended the SQ thermodynamic

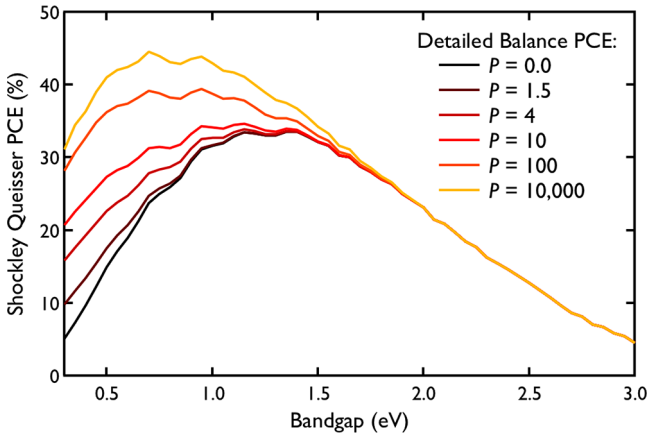

FIGURE 4. The detailed balance-derived maximum allowable PCE.

analysis to demonstrate that the same high conversion efficiency possible from a multijunction solar cell could be obtained by utilizing the total excess kinetic energy of hot photogenerated carriers in a single bandgap device where hot carriers are transported and collected at energy-selective contacts.[37,38]

Record solar cell efficiencies have not reached these fundamental limits but are asymptotically approaching them. For example, the record efficiency for c-Si is 25%, while for GaAs, the record is 28.3%.[43] The record one-sun triple-junction solar cell has an efficiency of 34.1%.[44] Under optical concentration, the efficiency increases, and the record for all PV cells is 43.5% at 418 suns.[44] Currently, these high efficiency cells (including the single-junction cells) do not meet the criteria of TGPV because the module cost is far too high. However, under concentration, the module costs can be transferred to less expensive concentrating optics. Inexpensive tandem cells based on solution-processed QDs[45,46] or organic PV materials[47] are being explored and with improvement may become a viable TGPV technology.[48]

The MEG approach yields a lower thermodynamic conversion efficiency of about 45% compared with the hot-carrier solar cell; this results from energy loss in the former between integer multiples of the bandgap energy starting at $1E_g$. However, the MEG approach is particularly attractive because only one absorber layer is needed, conventional carrier contacts can be employed, and the cell can be fabricated mainly using solution-processing techniques. Figure 4 shows detailed balance calculations following the SQ approach for various values of P. Black represents the conventional SQ calculation with just one e−h pair created per photon and thus $P = 0$. The yellow curve for $P = 10\,000$ achieves the maximum multiplication energetically allowed. Significant improvements in P are needed in practical

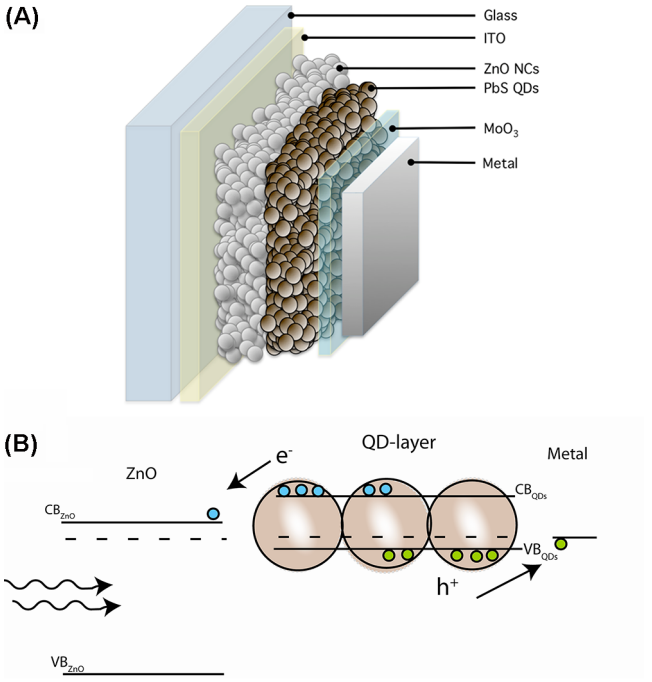

FIGURE 5. (a) A common structure for QD solar cells where the QD layer (PbS in this case) forms a heterojunction with ZnO to extract electrons through the ITO electrode. The holes are collected at the back of the film, often by a transition metal oxide-modified (MoO_3, in this case) metal electrode. The energetics (b) are often approximated by a traditional semiconductor formalism with a single conduction and valence band for electrons and holes. However at this stage, little is known about the details of the potential distribution of these nanocrystalline interfaces.

materials to greatly impact PCEs from MEG. PbSe QRs,[29] InP QDs, (6,5)-SWCNT,[49] and Si QDs[50] are all in the range of 1−10, where useful improvements in PCE begin to occur.

Strategies for Quantum Dot Solar Cells

There are several design strategies to incorporate MEG-active materials in practical solar cells:[51]

(1) The QDs can be in contact with and allow other media that facilitate charge separation and transport, such as a QD-sensitized semiconductor solar cell (QDSSC)[52,53] or dispersion into conducting polymer matrices.[54]

(2) The QDs form conductive arrays used in standard thin film solar cell architectures (such as Schottky, heterojunction, or p−i−n configurations).

(3) The QDs remain in an electrically insolated environment and undergo energy transfer into suitable energy acceptors where charges are separated.[55]

Here we discuss approaches based on implementing strategy 2 where a QD absorber layer is the light absorbing component of the solar cell. The planar heterojunction variety

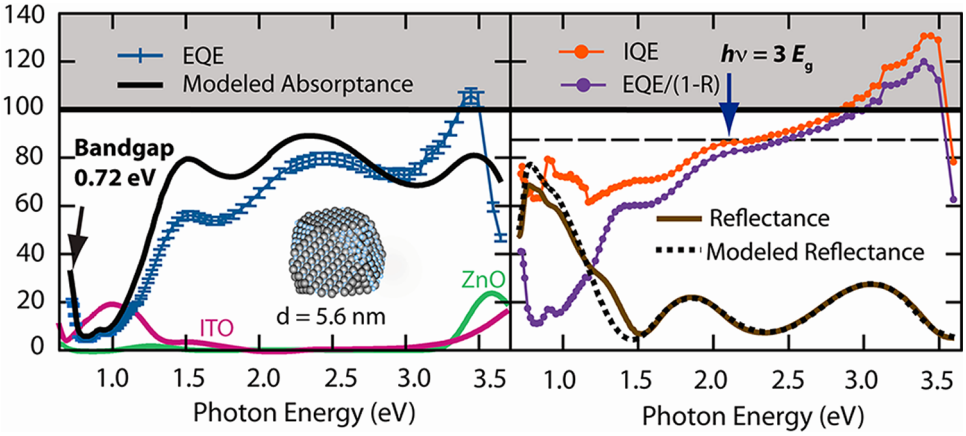

FIGURE 6. (left panel) EQE (blue curve) for a 0.72 eV bandgap PbSe QD solar cell and the absorptance of ZnO (green), ITO (purple), and the QD layer (black). (right panel) The measured (brown) and modeled (dotted) device reflectance. The EQE/(1 − *R*) (purple) is a first estimate of the IQE. An optical model of the entire device stack was used to determine the IQE (orange). The IQE curve exhibits a rise from ~85% to its maximum of 130% near $3E_g$. Light exceeding 3.5 eV is blocked by glass, ITO, and ZnO. Reproduced with permission from ref 71. Copyright 2011 AAAS.

of this approach, in particular, has shown marked progress in PCE.[56−61] A prototypical heterojunction QD solar cell is shown schematically in Figure 5a with an approximate band diagram (Figure 5b). The basic strategy is to sandwich a QD-layer between an n-type window layer that accepts electrons while blocking holes and a metal electrode that accepts holes. Light is absorbed in the QDs and excitons separate to form free electrons and holes. Electrons flow toward the n-type layer, and holes are collected at the metal electrode. Critical issues that need to be addressed are formation of the QD layer and its front and back interfaces. The QD layer must promote facile exciton dissociation and subsequent e−h transport, while the interfaces need optimal energetics to selectively extract charge carriers.

In colloidal PbSe QD synthesis, organic ligands, typically oleic acid, are used to control growth kinetics and allow for stable colloidal dispersions, however, they electrically isolate the QDs, thus preventing exciton dissociation and charge conduction. Exposure of a dry QD film to short molecules with high affinity to bond with Pb (such as short alkane thiols, amines, or carboxylic acids)[62] removes the ligands and reduces the distance between QD cores. Solid-state ligand exchange is typically done in a layer-by-layer fashion, producing thick, pinhole free layers that are conductive and can withstand evaporation of a large area metal contact without electrically shunting the film. The charge transport through the QD films remains an intriguing scientific challenge that has attracted intense research effort.[62−66] Recently CdSe QD films treated with ammonium thiocyanate followed by diffusion of In metal displayed record carrier mobilities of 27 $cm^2\ V^{-1}\ s^{-1}$.[67] In a separate approach using short *inorganic* ligands, carrier mobilities have reached ~15 $cm^2\ V^{-1}\ s^{-1}$.[68]

Chemical treatments to form conductive QD films can potentially affect MEG production in negative ways. Changes in the surface chemistry affect QD−ligand interactions that could subsequently alter exciton-cooling rates.[8,9] A few studies have attempted to address this concern[69,70] and found that the single-exciton lifetimes decrease, reflecting an increased rate of recombination; the biexciton lifetime increases for decreasing QD−QD separation; and the absorption cross section per QD increases for films with longer biexciton lifetimes. TA results also suggested that MEG is nearly quenched in PbSe QD films when treated with 1,2-ethanedithiol (EDT). Similarly, although Schottky-junction devices utilizing this treatment perform reasonably well, no conclusive evidence for collection of multiple carriers per absorbed photon was found. However, it is possible that both the photocurrent measurements and the TA underestimate MEG in these experiments. The biexciton lifetimes showed departure from simple exciton−exciton interactions within individual QDs. Strong QD−QD coupling allows for excitons in adjacent QDs to interact. At low fluences, this can modify the first-exicton dynamics and in particular the Auger recombination dynamics used to quantify MEG, rendering it more complicated to extract a meaningful QY. Thus, more work is necessary to unravel the complex dynamics within highly coupled QD films. Compared with earlier Schottky-junction cells, the heterojunction architecture depicted in Figure 5 extracts electrons at the incident side of the QD film rather than the back contact. This aids the extraction of

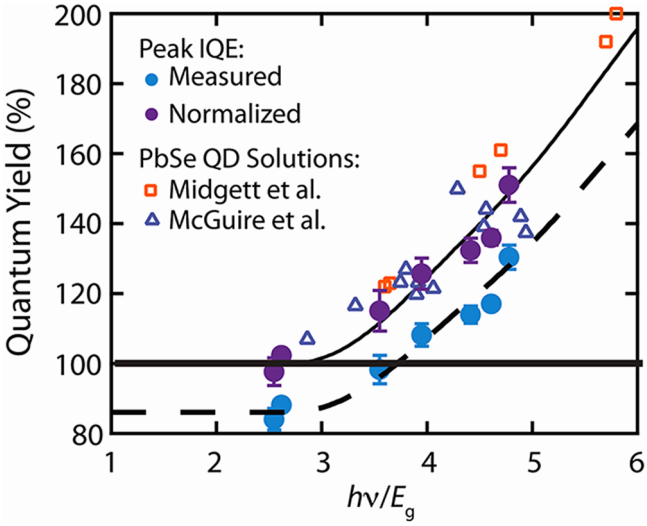

FIGURE 7. Peak IQE values from devices composed of seven different QD sizes. The peak IQE values are corrected for intrinsic losses in the solar cell (estimated at ~15%). The hollow triangles and squares represent ultrafast transient absorption measurements of PbSe QD solutions taken from refs 19 and 21, respectively. Reproduced with permission from ref 71. Copyright 2011 AAAS.

charge carriers produced from high-energy photons (those capable of undergoing MEG).

Observation of MEG in a PbSe Quantum Dot Solar Cell

Using a modified device structure as shown in Figure 5, we measured the EQE for photocurrent in QD solar cells using various sizes of PbSe QDs with bandgap ranging from 0.7 to 1.5 eV.[71] The QD-layer is initially deposited using a layer-by-layer EDT treatment followed by an additional hydrazine treatment of the QD films that allows use of smaller bandgap QDs by increasing the V_{oc} and shunt resistance within the device. Figure 6 displays EQE (left panel, blue curve) for a device with QD bandgap of 0.72 eV. The first exciton absorption peak is visible at the red edge of our EQE spectrometer and other broad features are a result of optical interference that occurs in a dielectric stack (here consisting of ITO/ZnO/PbSe QDs/Au). Despite reflection and absorption by the glass, ITO, and ZnO layers, this device exhibited an EQE of 106% ± 3% for photons with 3.44 eV (~$4E_g$). An antireflection coating increases the peak EQE to ~114%. To our knowledge, this is the first solar cell to exhibit an external or internal QY > 100% with photons within the solar spectrum. In order to compare the photocurrent measurements to the ultrafast spectroscopy data, the internal quantum efficiency (IQE) of the device was determined. The IQE is determined by dividing the EQE by the calculated combined absorptance of the ZnO and PbSe layers $A = A_{PbSe} + A_{ZnO}$. In Figure 7, we compare the photocurrent measurements to the TA measurements and find reasonable agreement to confirm previous TA measurements.

Conclusions and Future Challenges

Quantum dot solar cells remain a promising technology for inexpensive, scalable, and efficient solar cells. Thanks to their size and surface tunability and solution processing, it should be possible to make inexpensive and efficient devices from inks. The challenge is to increase the MEG efficiency so as to approach the energy conservation limit and to simultaneously improve the QD device performance. Promising avenues toward achieving the first goal have recently been demonstrated. Near staircase behavior has been reported in films of silicon QDs.[72] Colloidal solutions of Si QDs have also shown high MEG efficiencies,[50] while carbon nanotubes show MEG-like behavior.[73] Semiconductor nanocrystals offer many avenues toward increasing the MEG yields through internal and external modifications.

In addition to searching for ways to maximize MEG, an equivalent effort focusing on eliminating nonradiative recombination and increasing carrier mobility is of paramount importance in order to improve the photocurrent quantum yield in the visible and near-IR regions. In order to accomplish this, better transport and reduced recombination is necessary. The fact that the EQE exceeds 100% is a first step toward achieving a TGPV technology.

We gratefully acknowledge useful discussion with Aaron Midgett, Matt Law, Jianbo Gao, and Barbara Hughes. We also acknowledge helpful discussions and interactions with Alexander Efros and Victor Klimov. Our work on the photophysics and chemistry of isolated QDs is supported by the Solar Photochemistry program within the Division of Chemical Sciences, Geosciences, and Biosciences in the Office of Basic Energy of the Department of Energy. Incorporating the QDs into working solar cells and studying how the QDs couple to one another to form QD layers is supported by the Center for Advanced Solar Photophysics, an Energy Frontier Research Center funded by the U.S. Department of Energy, Office of Science, Office of Basic Energy Sciences. DOE funding was provided to NREL through Contract DE-AC36-086038308.

BIOGRAPHICAL INFORMATION

Matthew C. Beard graduated with a Ph.D. in Physical Chemistry in 2002 from Yale University and joined NREL in 2003. He is currently a Senior Scientist in the Chemistry and Materials Science Center.

His interest includes quantum dot solar cells, exciton and charge carrier dynamics in quantum dots, and coupled quantum dot films.

Joseph M. Luther holds a Ph.D. in Physics from Colorado School of Mines and is currently a Senior Scientist in the Chemical and Materials Science Center. His interests are in photovoltaic device design, optoelectronic properties of materials, and the synthesis of complex nanostructures.

Octavi E. Semonin received his B.A. in Physics from Harvey Mudd College in 2006. He graduated with a Ph.D. in Physics from the University of Colorado, Boulder, in 2012. In September 2012, he will join Columbia University to continue his research as an Energy Frontiers Research Center Fellow.

Arthur J. Nozik is a Professor Adjoint in the Department of Chemistry and Biochemistry at the University of Colorado, Boulder, the Senior Research Fellow Emeritus at the National Renewable Energy Laboratory (NREL), and a Founding Fellow of the recently formed NREL/University of Colorado Renewable and Sustainable Energy Institute (RASEI). Nozik received his BChE from Cornell University in 1959 and his Ph.D. in Physical Chemistry from Yale University in 1967. Professor Nozik's recent research interests include size quantization effects in semiconductor quantum dots and quantum wells, including multiple exciton generation from a single photon, and the applications of unique effects in nanostructures and nanoscience to advanced approaches for solar photon conversion to photovoltaic electricity and solar fuels.

FOOTNOTES

The authors declare no competing financial interest.

REFERENCES

1 Shockley, W.; Queisser, H. J. Detailed Balance Limit of Efficiency of p-n Junction Solar Cells. *J. Appl. Phys.* **1961**, *32*, 510–519.

2 Green, M. A. *Third Generation Photovoltaics*; Bridge Printery: Sydney, 2001.

3 Kang, I.; Wise, F. W. Electronic Structure and Optical Properties of PbS and PbSe Quantum Dots. *J. Opt. Soc. Am. B* **1997**, *14*, 1632–1646.

4 Kolodinski, S.; Werner, J. H.; Wittchen, T.; Queisser, H. J. Quantum Efficiencies Exceeding Unity Due to Impact Ionization in Silicon Solar-Cells. *Appl. Phys. Lett.* **1993**, *63*, 2405–2407.

5 Queisser, H. J. Multiple Carrier Generation in Solar Cells. *Sol. Energy Mater. Sol. Cells* **2010**, *94*, 1927–1930.

6 Wolf, M.; Brendel, R.; Werner, J. H.; Queisser, H. J. Solar Cell Efficiency and Carrier Multiplication in $Si_{1-x}Ge_x$ Alloys. *J. Appl. Phys.* **1998**, *83*, 4213–4221.

7 Blackburn, J. L.; Ellingson, R. J.; Micic, O. I.; Nozik, A. J. Electron Relaxation in Colloidal InP Quantum Dots with Photogenerated Excitons or Chemically Injected Electrons. *J. Phys. Chem. B* **2003**, *107*, 102–109.

8 Guyot-Sionnest, P.; Wehrenberg, B.; Yu, D. Intraband Relaxation in CdSe Nanocrystals and the Strong Influence of the Surface Ligands. *J. Chem. Phys.* **2005**, *123*, No. 074709.

9 Pandey, A.; Guyot-Sionnest, P. Slow Electron Cooling in Colloidal Quantum Dots. *Science* **2008**, *322*, 929–932.

10 Schaller, R. D.; Klimov, V. I. High Efficiency Carrier Multiplication in PbSe Nanocrystals: Implications for Solar Energy Conversion. *Phys. Rev. Lett.* **2004**, *92*, No. 186601.

11 Ellingson, R. J.; Beard, M. C.; Johnson, J. C.; Yu, P. R.; Micic, O. I.; Nozik, A. J.; Shabaev, A.; Efros, A. L. Highly Efficient Multiple Exciton Generation in Colloidal PbSe and PbS Quantum Dots. *Nano Lett.* **2005**, *5*, 865–871.

12 Schaller, R. D.; Sykora, M.; Jeong, S.; Klimov, V. I. High-Efficiency Carrier Multiplication and Ultrafast Charge Separation in Semiconductor Nanocrystals Studied via Time-Resolved Photoluminescence. *J. Phys. Chem. B* **2006**, *110*, 25332–25338.

13 Beard, M. C.; Ellingson, R. J. Multiple Exciton Generation in Semiconductor Nanocrystals: Toward Efficient Solar Energy Conversion. *Laser Photonics Rev.* **2008**, *2*, 377–399.

14 Nair, G.; Bawendi, M. G. Carrier Multiplication Yields of CdSe and CdTe Nanocrystals by Transient Photoluminescence Spectroscopy. *Phys. Rev. B: Condens. Matter Mater. Phys.* **2007**, *76*, No. 081304.

15 Nair, G.; Geyer, S. M.; Chang, L. Y.; Bawendi, M. G. Carrier Multiplication Yields in PbS and PbSe nanocrystals measured by transient Photoluminescence. *Phys. Rev. B: Condens. Matter Mater. Phys.* **2008**, *78*, 125325.

16 Pijpers, J. J. H.; Hendry, E.; Milder, M. T. W.; Fanciulli, R.; Savolainen, J.; Herek, J. L.; Vanmaekelbergh, D.; Ruhman, S.; Mocatta, D.; Oron, D.; Aharoni, A.; Banin, U.; Bonn, M. Carrier multiplication and its reduction by photodoping in colloidal InAs quantum dots. *J. Phys. Chem. C* **2008**, *112*, 4783–4784.

17 Ben-Lulu, M.; Mocatta, D.; Bonn, M.; Banin, U.; Ruhman, S. On the Absence of Detectable Carrier Multiplication in a Transient Absorption Study of InAs/CdSe/ZnSe Core/Shell1/Shell2 Quantum Dots. *Nano Lett.* **2008**, *8* (4), 1207–1211.

18 Beard, M. C. Multiple Exciton Generation in Semiconductor Quantum Dots. *J. Phys. Chem. Lett.* **2011**, *2*, 1282–1288.

19 McGuire, J. A.; Sykora, M.; Joo, J.; Pietryga, J. M.; Klimov, V. I. Apparent Versus True Carrier Multiplication Yields in Semiconductor Nanocrystals. *Nano Lett.* **2010**, *10*, 2049–2057.

20 Mcguire, J. A.; Joo, J.; Pietryga, J. M.; Schaller, R. D.; Klimov, V. I. New Aspects of Carrier Multiplication in Semiconductor Nanocrystals. *Acc. Chem. Res.* **2008**, *41*, 1810–1819.

21 Midgett, A. G.; Hillhouse, H. W.; Huges, B. K.; Nozik, A. J.; Beard, M. C. Flowing versus Static Conditions for Measuring Multiple Exciton Generation in PbSe Quantum Dots. *J. Phys. Chem. C* **2010**, *114*, 17486–17500.

22 Beard, M. C.; Midgett, A. G.; Hanna, M. C.; Luther, J. M.; Hughes, B. K.; Nozik, A. J. Comparing Multiple Exciton Generation in Quantum Dots To Impact Ionization in Bulk Semiconductors: Implications for Enhancement of Solar Energy Conversion. *Nano Lett.* **2010**, *10*, 3019–3027.

23 Bertazzi, F.; Moresco, M.; Penna, M.; Goano, M.; Bellotti, E. Full-Band Monte Carlo Simulation of HgCdTe APDs. *J. Electron. Mater.* **2010**, *39*, 912–917.

24 Tirino, L.; Weber, M.; Brennan, K. F.; Bellotti, E.; Goano, M. Temperature Dependence of the Impact Ionization Coefficients in GaAs, Cubic SiC, and Zinc-Blende GaN. *J. Appl. Phys.* **2003**, *94*, 423–430.

25 Ziaja, B.; London, R. A.; Hajdu, J. Ionization by Impact Electrons in Solids: Electron Mean Free Path Fitted over a Wide Energy Range. *J. Appl. Phys.* **2006**, *99*, No. 033514.

26 Ridley, B. K. *Quantum Processes in Semiconductors*; Oxford University Press: New York, 1988.

27 Alig, R. C.; Bloom, S. Electron-Hole-Pair Creation Energies in Semiconductors. *Phys. Rev. Lett.* **1975**, *35*, 1522–1525.

28 Pijpers, J. J. H.; Ulbricht, R.; Tielrooij, K. J.; Osherov, A.; Golan, Y.; Delerue, C.; Allan, G.; Bonn, M. Assessment of Carrier-Multiplication Efficiency in Bulk PbSe and PbS. *Nat. Phys.* **2009**, *5*, 811–814.

29 Cunningham, P. D.; Boercker, J. B.; Foos, E.; Lumb, M. P.; Smith, A. R.; Tischler, J. G.; Melinger, J. S. Enhanced Multiple Exciton Generation in Quasi-One-Dimensional Semiconductors. *Nano Lett.* **2011**, *11*, 3476–3481.

30 Baer, R.; Rabani, E. Expeditious Stochastic Calculation of Multiexciton Generation Rates in Semiconductor Nanocrystals. *Nano Lett.* **2012**, *12*, 2123–2128.

31 Lin, Z. B.; Franceschetti, A.; Lusk, M. T. Size Dependence of the Multiple Exciton Generation Rate in CdSe Quantum Dots. *ACS Nano* **2011**, *5*, 2503–2511.

32 Bartnik, A. C.; Efros, A. L.; Koh, W. K.; Murray, C. B.; Wise, F. W. Electronic States and Optical Properties of PbSe Nanorods and Nanowires. *Phys. Rev. B: Condens. Matter Mater. Phys.* **2010**, *82*, No. 195313.

33 Witzel, W. M.; Shabaev, A.; Hellberg, C. S.; Jacobs, V. L.; Efros, A. L. Quantum Simulation of Multiple-Exciton Generation in a Nanocrystal by a Single Photon. *Phys. Rev. Lett.* **2010**, *105*, No. 137401.

34 Shabaev, A.; Efros, A. L.; Nozik, A. J. Multiexciton Generation by a Single Photon in Nanocrystals. *Nano Lett.* **2006**, *6*, 2856–2863.

35 Stewart, J. T.; Padilha, L. A.; Qazilbash, M. M.; Pietryga, J. M.; Midgett, A. G.; Luther, J. M.; Beard, M. C.; Nozik, A. J.; Klimov, V. I. Comparison of Carrier Multiplication Yields in PbS and PbSe Nanocrystals: The Role of Competing Energy-Loss Processes. *Nano Lett.* **2012**, *12*, 622–628.

36 De Vos, A. Detailed Balance Limit of the Efficiency of Tandem Solar Cells. *J. Phys. D: Appl. Phys.* **1980**, *13*, 839–846.

37 Konig, D.; Casalenuovo, K; Takeda, Y; Conibeer, G. J.; Guillemoles, J. F.; Patterson, R.; Huang, L. M.; Green, M. A. Hot Carrier Solar Cells: Principles, materials, and design. *Phys. E (Amsterdam, Neth.)* **2010**, *42*, 2862–2866.

38 Takeda, Y.; Motohiro, T.; Konig, D.; Aliberti, P.; Feng, Y.; Shrestha, S.; Conibeer, G. Practical Factors Lowering Conversion Efficiency of Hot Carrier Solar Cells. *Appl. Phys. Express* **2010**, *3*, No. 104301.

39 Trupke, T.; Green, M. A.; Wurfel, P. Improving Solar Cell Efficiencies by Up-Conversion of Sub-Band-Gap Light. *J. Appl. Phys.* **2002**, *92*, 4117–4122.

40 Trupke, T.; Green, M. A.; Wurfel, P. Improving Solar Cell Efficiencies by Down-Conversion of High-Energy Photons. *J. Appl. Phys.* **2002**, *92*, 1668–1674.

41 Hanna, M. C.; Nozik, A. J. Solar Conversion Efficiency of Photovoltaic and Photoelectrolysis Cells with Carrier Multiplication Absorbers. *J. Appl. Phys.* **2006**, *100*, No. 074510.

42 Ross, R. T.; Nozik, A. J. Efficiency of Hot-Carrier Solar-Energy Converters. *J. Appl. Phys.* **1982**, *53*, 3813–3818.

43 Yablonovitch, E.; Miller, O. D. The Opto-Electronics which Broke the Efficiency Record in Solar Cells. *CLEO: Sci. Innovation* 2012, No. CF2J.1.

44 Green, M. A.; Emery, K.; Hishikawa, Y.; Warta, W.; Dunlop, E. D. Solar Cell Efficiency Tables (version 39). *Prog. Photovoltaics* **2012**, *20*, 12–20.

45 Wang, X.; Koleilat, G. I.; Tang, J.; Liu, H.; Kramer, I. J.; Debnath, R.; Brzozowski, L.; Barkhouse, D. A. R.; Levina, L.; Hoogland, S.; Sargent, E. H. Tandem Colloidal Quantum Dot Solar Cells Employing a Graded Recombination Layer. *Nat. Photonics* **2011**, *5*, 480–484.

46 Choi, J. J.; Wenger, W. N.; Hoffman, R. S.; Lim, Y. F.; Luria, J.; Jasieniak, J.; Marohn, J. A.; Hanrath, T. Solution-Processed Nanocrystal Quantum Dot Tandem Solar Cells. *Adv. Mater.* **2011**, *23*, 3144–3148.

47 Ameri, T.; Dennler, G.; Lungenschmied, C.; Brabec, C. J. Organic Tandem Solar Cells: A Review. *Energ Environ Sci.* **2009**, *2*, 347–363.

48 Heliatek. Heliatek Sets new world record efficiency of 10.7% for its organic tandem cell. http://www.heliatek.com/newscenter/latest_news/heliatek-erzielt-mit-107-effizienz-neuen-weltrekord-fur-seine-organische-tandemzelle/?lang=en. Accessed October 2012.

49 Wang, S. J.; Khafizov, M.; Tu, X. M.; Zheng, M.; Krauss, T. D. Multiple Exciton Generation in Single-Walled Carbon Nanotubes. *Nano Lett.* **2010**, *10*, 2381–2386.

50 Beard, M. C.; Knutsen, K. P.; Yu, P. R.; Luther, J. M.; Song, Q.; Metzger, W. K.; Ellingson, R. J.; Nozik, A. J. Multiple Exciton Generation in Colloidal Silicon Nanocrystals. *Nano Lett.* **2007**, *7*, 2506–2512.

51 Nozik, A. J. Quantum Dot Solar Cells. *Phys. E (Amsterdam, Neth.)* **2002**, *14*, 115–120.

52 Kamat, P. V. Quantum Dot Solar Cells. Semiconductor Nanocrystals as Light Harvesters. *J. Phys. Chem. C* **2008**, *112*, 18737–18753.

53 Sambur, J. B.; Novet, T.; Parkinson, B. A. Multiple Exciton Collection in a Sensitized Photovoltaic System. *Science* **2010**, *330*, 63–66.

54 Dayal, S.; Kopidakis, N.; Olson, D. C.; Ginley, D. S.; Rumbles, G. Photovoltaic Devices with a Low Band Gap Polymer and CdSe Nanostructures Exceeding 3% Efficiency. *Nano Lett.* **2010**, *10*, 239–242.

55 Achermann, M.; Petruska, M. A.; Kos, S.; Smith, D. L.; Koleske, D. D.; Klimov, V. I. Energy-Transfer Pumping of Semiconductor Nanocrystals Using an Epitaxial Quantum Well. *Nature* **2004**, *429*, 642–646.

56 Choi, J. J.; Lim, Y.-F.; Santiago-Berrios, M. B.; Oh, M.; Hyun, B.-R.; Sun, L.; Bartnik, A. C.; Goedhart, A.; Malliaras, G. G.; Abruña, H. D.; Wise, F. W.; Hanrath, T. PbSe Nanocrystal Excitonic Solar Cells. *Nano Lett.* **2009**, *9*, 3749–3755.

57 Leschkies, K. S.; Beatty, T. J.; Kang, M. S.; Norris, D. J.; Aydil, E. S. Solar Cells Based on Junctions between Colloidal PbSe Nanocrystals and Thin ZnO Films. *ACS Nano* **2009**, *3*, 3638–3648.

58 Ma, W. L.; Swisher, S. L.; Ewers, T.; Engel, J.; Ferry, V. E.; Atwater, H. A.; Alivisatos, A. P. Photovoltaic Performance of Ultrasmall PbSe Quantum Dots. *ACS Nano* **2011**, *5*, 8140–8147.

59 Luther, J. M.; Gao, J. B.; Lloyd, M. T.; Semonin, O. E.; Beard, M. C.; Nozik, A. J. Stability Assessment on a 3% Bilayer PbS/ZnO Quantum Dot Heterojunction Solar Cell. *Adv. Mater.* **2010**, *22*, 3704–3707.

60 Tang, J.; Brzozowski, L.; Barkhouse, D. A. R.; Wang, X.; Debnath, R.; Wolowiec, R.; Palmiano, E.; Levina, L.; Pattantyus-Abraham, A. G.; Jamakosanovic, D.; Sargent, E. H. Quantum Dot Photovoltaics in the Extreme Quantum Confinement Regime: The Surface-Chemical Origins of Exceptional Air- and Light-Stability. *ACS Nano* **2010**, *4*, 869–878.

61 Gao, J. B.; Perkins, C. L.; Luther, J. M.; Hanna, M. C.; Chen, H. Y.; Semonin, O. E.; Nozik, A. J.; Ellingson, R. J.; Beard, M. C. n-Type Transition Metal Oxide as a Hole Extraction Layer in PbS Quantum Dot Solar Cells. *Nano Lett.* **2011**, *11*, 3263–3266.

62 Liu, Y.; Gibbs, M.; Puthussery, J.; Gaik, S.; Ihly, R.; Hillhouse, H. W.; Law, M. Dependence of Carrier Mobility on Nanocrystal Size and Ligand Length in PbSe Nanocrystal Solids. *Nano Lett.* **2010**, *10*, 1960–1969.

63 Houtepen, A. J.; Kockmann, D.; Vanmaekelbergh, D. Reappraisal of Variable-Range Hopping in Quantum-Dot Solids. *Nano Lett.* **2008**, *8*, 3516–3520.

64 Mentzel, T. S.; Porter, V. J.; Geyer, S.; MacLean, K.; Bawendi, M. G.; Kastner, M. A. Charge Transport in PbSe Nanocrystal Arrays. *Phys. Rev. B: Condens. Matter Mater. Phys.* **2008**, *77*, No. 075316.

65 Wehrenberg, B. L.; Yu, D.; Ma, J. S.; Guyot-Sionnest, P. Conduction in Charged PbSe Nanocrystal Films. *J. Phys. Chem. B* **2005**, *109*, 20192–20199.

66 Talapin, D. V.; Murray, C. B. PbSe Nanocrystal Solids for n- and p-Channel Thin Film Field-Effect Transistors. *Science* **2005**, *310*, 86–89.

67 Choi, J. H.; Fafarman, A. T.; Oh, S. J.; Ko, D. K.; Kim, D. K.; Diroll, B. T.; Muramoto, S.; Gillen, J. G.; Murray, C. B.; Kagan, C. R. Bandlike Transport in Strongly Coupled and Doped Quantum Dot Solids: A Route to High-Performance Thin-Film Electronics. *Nano Lett.* **2012**, *12*, 2631–2638.

68 Lee, J. S.; Kovalenko, M. V.; Huang, J.; Chung, D. S.; Talapin, D. V. Band-Like Transport, High Electron Mobility and High Photoconductivity in All-Inorganic Nanocrystal Arrays. *Nat Nanotechnol.* **2011**, *6*, 348–352.

69 Luther, J. M.; Beard, M. C.; Song, Q.; Law, M.; Ellingson, R. J.; Nozik, A. J. Multiple Exciton Generation in Films of Electronically Coupled PbSe Quantum Dots. *Nano Lett.* **2007**, *7*, 1779–1784.

70 Beard, M. C.; Midgett, A. G.; Law, M.; Semonin, O. E.; Ellingson, R. J.; Nozik, A. J. Variations in the Quantum Efficiency of Multiple Exciton Generation for a Series of Chemically Treated PbSe Nanocrystal Films. *Nano Lett.* **2009**, *9*, 836–845.

71 Semonin, O. E.; Luther, J. M.; Choi, S.; Chen, H. Y.; Gao, J. B.; Nozik, A. J.; Beard, M. C. Peak External Photocurrent Quantum Efficiency Exceeding 100% via MEG in a Quantum Dot Solar Cell. *Science* **2011**, *334*, 1530–1533.

72 Trinh, M. T.; Limpens, R.; de, B.; WDAM; Schins, J. M.; Siebbeles, L. D. A.; Gregorkiewicz, T. Direct Generation of Multiple Excitons in Adjacent Silicon Nanocrystals Revealed by Induced Absorption. *Nat. Photonics* **2012**, *6*, 316–321.

73 Gabor, N. M.; Zhong, Z. H.; Bosnick, K.; Park, J.; McEuen, P. L. Extremely Efficient Multiple Electron-Hole Pair Generation in Carbon Nanotube Photodiodes. *Science* **2009**, *325*, 1367–1371.